

***UNCARIA GAMBIR AS NATURAL CORROSION INHIBITOR
FOR MILD STEEL IN ACIDIC SOLUTION***

MOHD. HAZWAN HUSSIN

**UNIVERSITI SAINS MALAYSIA
2010**

DECLARATION

Saya mengisyiharkan bahawa kandungan yang dibentangkan di dalam tesis ini adalah hasil kerja saya sendiri dan telah dijalankan di Universiti Sains Malaysia. Tesis ini juga tidak pernah diserahkan untuk ijazah yang lain sebelum ini.

I declare that the content which is presented in this thesis is my own work and has been done at Universiti Sains Malaysia. This thesis has not been previously submitted for any other degree.

Disaksikan oleh:

Witnessed by:

Tandatangan Calon:

Signature of Candidate:

Nama Calon:

Mohd. Hazwan Hussin

Name of Candidate:

NRIC/Passport No.:

861223-23-5283

Tandatangan Saksi:

Signature of Witness:

Nama Saksi:

Prof Madya Dr. Mohd. Jain
Noordin Mohd. Kassim

Name of Witness:

NRIC/Passport No.:

540905-10-5657

***UNCARIA GAMBIR AS NATURAL CORROSION INHIBITOR
FOR MILD STEEL IN ACIDIC SOLUTION***

by

MOHD. HAZWAN HUSSIN

**Thesis submitted in fulfilment of the
requirement for the degree
of Master of Science**

September 2010

ACKNOWLEDGEMENTS

In the name of God, the most compassionate, the most merciful. Hereby, I would like to acknowledge individuals that strongly helped and supported me throughout this research. First and foremost, I would like to thank my supervisor Assoc. Prof. Dr. Mohd. Jain Noordin Mohd. Kassim for his outstanding guidance, advice, encouragement and assistance.

Also, a special thanks to Ministry of Higher Education for the scholarship given under Biasiswa Bajet Mini and to Universiti Sains Malaysia for the Graduate Assistant scheme and Research University-Postgraduate Research Grant Scheme (RU-PRGS: 1001/PKIMIA/831016). Without this financial support, it must be a hard scramble problem for me to finish this degree or research.

My gratitude also goes to all the administrative and technical staff of School of Chemical Sciences (En. Ali and En. Sobri), School of Biological Sciences (especially to Electron Microscope Unit, Pn. Jamilah and En. Johari) and School of Material, Mineral and Resource Engineering (especially to Petrology and Chemical Lab: XRF elemental analysis, Pn. Fong Lee Lee).

Lastly, my sincere appreciation goes to all my lab mates (Kim Suan, Lean Seey, Rozaini, Kang Wei, Azraa, Wani, Aim, Hairul and Awin), friends (Nofrizal, Salmiah and Affaizza), lecturers and family in Johore. Mum and Dad, you're the strength and the driving force for me to complete my Master's degree. Thank you.

Mohd. Hazwan Hussin

September 2010

TABLE OF CONTENTS

	Page
Acknowledgements	ii
Table of contents	iii
List of Figures	vii
List of Tables	x
List of Abbreviations	xii
Abstract	xiv
Abstrak	xvi
CHAPTER 1 – INTRODUCTION	1
1.1 Introduction to Corrosion	1
1.1.1 Corrosion in definitions	2
1.1.2 Corrosion of iron	3
1.1.3 Consequences of corrosion	6
1.2 Corrosion protection	7
1.3 Corrosion inhibitors	9
1.3.1 The inhibitors	11
1.3.2 Corrosion inhibition of mild steel in acidic solution	13
1.3.3 Methods for corrosion inhibition study	14
1.3.3.1 Weight loss measurement	15
1.3.3.2 Potentiodynamic polarization measurement	17
1.3.3.3 Electrochemical impedance spectroscopy (EIS)	23
1.3.4 Characterization of metal surfaces	29

1.3.5	Adsorption process in corrosion inhibition	30
1.3.5.1	Types of adsorption process	31
1.3.5.2	Adsorption isotherm	32
1.4	<i>Uncaria gambir</i>	34
1.4.1	Gambir cube and its specifications	35
1.4.2	Previous studies of gambir	36
1.5	Catechin	38
1.5.1	Analysis of catechin	40
1.6	Objectives	41

CHAPTER 2 – EXPERIMENTAL		42
2.1	Material and preliminary tests	42
2.2	Gambir extraction	43
2.3	Characterization of gambir extract by Fourier Transform Infrared Spectroscopy (FTIR)	43
2.4	Assays for condensed tannins, total phenols and total flavonoid of gambir extract	45
2.4.1	Determination of condensed tannins by vanillin assay	45
2.4.2	Determination of total phenol by Folin-Ciocalteau assay	46
2.4.3	Determination of total flavonoid by Stiasny Test	46
2.5	Quantification of catechin content in gambir extract by HPLC	47
2.5.1	Qualitative determination of flavonoids	47
2.5.2	Quantitative determination of catechin	48
2.6	Mild steel elemental analysis by X-Ray Fluorescence (XRF)	48
2.7	Corrosion inhibition of gambir extract	49
2.7.1	The concentration effect of mild steel corrosion inhibition in	49

1 M HCl	
2.7.1.1 Weight loss measurement	50
2.7.1.2 Electrochemical measurements	50
2.7.1.2.1 Potentiodynamic polarization	51
2.7.1.2.2 Electrochemical impedance spectroscopy (EIS)	52
2.7.2 The temperature effect of mild steel corrosion inhibition in 1 M HCl	54
2.7.3 Adsorption isotherm and free Gibbs energy, ΔG_{ads}	54
2.7.4 Determination of potential zero charge (PZC)	54
2.7.5 Surface analysis	55
CHAPTER 3 – RESULT AND DISCUSSION	56
3.1 Characteristic of gambir	56
3.2 Gambir extraction	60
3.3 Characterization of gambir extract by Fourier Transform Infrared Spectroscopy (FTIR)	64
3.4 Assays for condensed tannins, total phenols and total flavonoid of gambir extract	69
3.4.1 Determination of condensed tannins by vanillin assay	69
3.4.2 Determination of total phenol by Folin-Ciocalteau assay	71
3.4.3 Determination of total flavonoid by Stiasny Test	73
3.5 Quantification of catechin content in gambir extract by HPLC	76
3.5.1 Qualitative determination of flavonoids	77
3.5.2 Quantitative determination of catechin	80
3.6 Mild steel elemental analysis by X-Ray Fluorescence (XRF)	81
3.7 Corrosion inhibition of ethyl acetate gambir extract	82

3.7.1	The concentration effect of mild steel corrosion inhibition in 1 M HCl	82
3.7.1.1	Weight loss measurement	82
3.7.1.2	Electrochemical measurements	87
3.7.1.2.1	Potentiodynamic polarization	87
3.7.1.2.2	Electrochemical impedance spectroscopy (EIS)	96
3.7.2	The temperature effect of mild steel corrosion inhibition in 1 M HCl	106
3.7.3	Adsorption isotherm and free Gibbs energy, ΔG_{ads}	113
3.7.4	Potential zero charge (PZC) and the mechanism of corrosion inhibition in 1 M HCl	120
3.7.5	Surface analysis	127
CHAPTER 4 – CONCLUSION		130
CHAPTER 5 – FUTURE RESEARCH RECOMMENDATIONS		134
REFERENCES		135
LIST OF PUBLICATIONS , SEMINARS/CONFERENCE AND AWARDS		147
APPENDICES		150

LIST OF FIGURES

	Page
Figure 1.1 The corrosion cycle of steel.	3
Figure 1.2 Electrochemical mechanism of corrosion of iron.	4
Figure 1.3 Pourbaix diagram for iron showing how corrosion protection can be achieved by using measures that bring a corroding system into either the immunity or the passivity region.	8
Figure 1.4 Typical weight loss measurement setup with metal being stand (left-hand side) and hanged (right-hand side).	15
Figure 1.5 Schematic activation free energy distribution.	19
Figure 1.6 A hypothetical Tafel plot.	22
Figure 1.7 The voltage-current phase angle.	25
Figure 1.8 A typical Nyquist plot.	26
Figure 1.9 A typical Bode plot.	27
Figure 1.10 The common electrochemical circuit used in a corrosion study.	27
Figure 1.11 <i>Uncaria gambir</i> plant.	35
Figure 1.12 The chemical structure of catechin.	39
Figure 2.1 Gambir extraction with different solvents.	44
Figure 2.2 Three conjunction electrode cell for potentiodynamic polarization measurement.	53
Figure 2.3 The electrochemical cell for the electrochemical impedance spectroscopy measurement.	53
Figure 3.1 The suggested hydrogen bond formation between the interaction of catechin and water.	58
Figure 3.2 The summary of gambir extraction.	63
Figure 3.3 FTIR spectra for (+)-catechin hydrate.	66
Figure 3.4 FTIR spectra for ground gambir (raw).	67

Figure 3.5	The infrared spectra of; a) standard (+)-catechin hydrate, b) 70 % aq. acetone, c) ethyl acetate, d) methanol, e) ethanol gambir extract.	68
Figure 3.6	The reaction mechanism of vanillin with condensed tannins.	69
Figure 3.7	Calibration curve of the absorbance at λ_{\max} 500 nm versus the concentration of (\pm)-catechin.	70
Figure 3.8	Non-corrected calibration curve of the absorbance at λ_{\max} 765 nm versus the concentration of gallic acid.	72
Figure 3.9	The suggested reaction of catechin with formaldehyde (Yeut Lan, 2006).	74
Figure 3.10	The program of gradient elution for separation of flavonoid standard.	76
Figure 3.11	The HPLC chromatogram of five flavonoid standards mixture.	77
Figure 3.12	The HPLC chromatogram of raw gambir.	78
Figure 3.13	The chemical structure of; (a) gallocatechin and (b) epigallocatechin gallate.	79
Figure 3.14	The calibration curve of standard (+)-catechin hydrate by HPLC-UV system.	80
Figure 3.15	The correlation of inhibition efficiency with concentration for both inhibitors at 303 K.	84
Figure 3.16	The correlation of corrosion rate with concentration for both inhibitors at 303 K.	85
Figure 3.17	Colour changes after 24 hours of immersion.	86
Figure 3.18	Tafel plot of mild steel in 1 M HCl and in the presence of different concentrations of ethyl acetate gambir extract (EAG) at 303 K.	89
Figure 3.19	Tafel plot of mild steel in 1 M HCl and in the presence of different concentrations of (+)-catechin hydrate (CH) at 303 K.	90
Figure 3.20	Nyquist plot of mild steel in 1 M HCl and in the presence of ethyl acetate gambir extract (EAG) at 303 K.	98
Figure 3.21	Nyquist plot of mild steel in 1 M HCl and in the presence of (+)-catechin hydrate (CH) at 303 K.	99

Figure 3.22	The Randle's CPE equivalent circuit.	100
Figure 3.23	Bode plot of mild steel in 1 M HCl and in the presence of ethyl acetate gambir extract (EAG).	104
Figure 3.24	Bode plot of mild steel in 1 M HCl and in the presence of (+)-catechin hydrate (CH).	105
Figure 3.25	Arrhenius plots for log CR versus 1/T for mild steel in 1 M HCl at different concentrations of EAG (above) and CH (below).	109
Figure 3.26	Transition state plot for log CR/T versus 1/T for mild steel in 1 M HCl at different concentrations of EAG (above) and CH (below).	111
Figure 3.27	Langmuir adsorption isotherm plot for ethyl acetate gambir extract (above) and (+)-catechin hydrate (below) in 1 M HCl at 303 K.	115
Figure 3.28	Frumkin adsorption isotherm plot for ethyl acetate gambir extract (above) and (+)-catechin hydrate (below) in 1 M HCl at 303 K.	116
Figure 3.29	Temkin adsorption isotherm plot for ethyl acetate gambir extract (above) and (+)-catechin hydrate (below) in 1 M HCl at 303 K.	117
Figure 3.30	Relation between conductivity and the applied potential on a steel electrode immersed in 1 M HCl without and with inhibitors.	123
Figure 3.31	The schematic illustration of different modes of adsorption on mild steel/1 M HCl interface.	125
Figure 3.32	SEM micrographs of a) untreated mild steel, b) mild steel without inhibitor in 1 M HCl, c) mild steel with 1000 ppm ethyl acetate gambir extract in 1 M HCl, d) mild steel with 1000 ppm (+)-catechin hydrate in 1 M HCl at magnification of 100 X.	129

LIST OF TABLES

		Page
Table 1.1	Circuit components in electrochemical impedance.	26
Table 1.2	The specification of gambir from National Indonesian Standard.	36
Table 3.1	The percentage of water content in gambir after drying for 1 hour at 105 °C.	57
Table 3.2	The solubility of gambir in different solvents.	59
Table 3.3	The percentage of residual impurities and lignin/fat content in gambir.	61
Table 3.4	Extraction yields of gambir by using different solvents at room temperature.	62
Table 3.5	The infrared adsorption band of samples.	65
Table 3.6	The content of condensed tannins determined by vanillin assay.	71
Table 3.7	The content of phenolic compound determined by Folin-Ciocalteau assay.	73
Table 3.8	The percentage of flavonoid in different gambir extracts.	75
Table 3.9	The content of catechin determined by HPLC method.	81
Table 3.10	The elemental compositions of mild steel determined by XRF analysis.	81
Table 3.11	The inhibition efficiency of mild steel in 1 M HCl with the presence of ethyl acetate gambir extract.	83
Table 3.12	The inhibition efficiency of mild steel in 1 M HCl with the presence of (+)-catechin hydrate.	83
Table 3.13	Polarization parameters for mild steel in 1 M HCl without and with different concentrations of ethyl acetate gambir extract (EAG) at 303 K.	91
Table 3.14	Polarization parameters for mild steel in 1 M HCl without and with different concentrations of (+)-catechin hydrate (CH) at 303 K.	92

Table 3.15	Electrochemical (EIS) parameters for mild steel in 1 M HCl without and with different concentrations of ethyl acetate gambir extract (EAG) at 303 K.	100
Table 3.16	Electrochemical (EIS) parameters for mild steel in 1 M HCl without and with different concentrations of (+)-catechin hydrate (CH) at 303 K.	100
Table 3.17	Effect of temperature on the mild steel corrosion in 1 M HCl for various concentrations of ethyl acetate gambir extract.	108
Table 3.18	Effect of temperature on the mild steel corrosion in 1 M HCl for various concentrations of (+)-catechin hydrate.	108
Table 3.19	Activation parameters of the dissolution reaction of mild steel in 1 M HCl in the absence and presence of ethyl acetate gambir extract.	110
Table 3.20	Activation parameters of the dissolution reaction of mild steel in 1 M HCl in the absence and presence of (+)-catechin hydrate.	110
Table 3.21	The calculated parameters from Langmuir Adsorption Isotherm for both inhibitors at 303 K.	120
Table 3.22	Values of E_r for the mild steel electrode in 1 M HCl for studied inhibitors.	122
Table 3.23	The percentage of element for each specimen in 1 M HCl obtained from the energy dispersive X-ray spectroscopy (EDX) analysis.	128

LIST OF ABBREVIATIONS

FTIR	Fourier Transfrom Infrared Spectroscopy
HPLC	High Performance Liquid Chromatography
EIS	Electrochemical Impedance Spectroscopy
SEM	Scanning Electron Microscopy
EDX	Energy Dispersive X-Ray Spectroscopy
XRF	X-Ray Fluorescence Spectroscopy
PZC	Potential Zero Charge
EAG	ethyl acetate gambir extract
CH	(+)-catechin hydrate
HCl	hydrochloric acid
GAE	gallic acid equivalent
CE	catechin equivalent
IE	inhibition efficiency
CR	corrosion rate
CPE	constant phase element
E_a	activation energy
ΔH	enthalpy
ΔS	entropy
ΔG_{ads}	Gibbs free energy of adsorption
ppm	parts per million
g	gram

mg	milligram
mL	millilitre
cm	centimetre
mm	millimetre
min	minutes
wt	weight
w/v	weight per volume
v/v	volume per volume
mV	millivolt
mV s^{-1}	millivolt per second
Hz	Hertz
kHz	kiloHertz
$\Omega \text{ cm}^2$	Ohm's centimetre square
mA cm^{-2}	milliampere per centimetre square
mpy	mils of penetration per year
mm y^{-1}	millimeters per year
E_{corr}	corrosion potential
E_r	Antropov 'rational' corrosion potential
I_{corr}	corrosion current density
R_p	polarization resistance
R_{ct}	resistance charge transfer
R_s	resistance solution

UNCARIA GAMBIR AS NATURAL CORROSION INHIBITOR FOR MILD STEEL IN ACIDIC SOLUTION

ABSTRACT

Uncaria gambir, a native Southeast Asia herbal plant has been characterized and studied as a mild steel corrosion inhibitor in acidic media. It was revealed that ethyl acetate gambir extract gave the highest condensed tannin, phenol and flavonoid content compared with other solvent extracts. Quantification studies by means of HPLC have shown that more than 80 % (wt) of gambir extract consists mainly of catechin. The effect of both ethyl acetate gambir extract and (+)-catechin hydrate as corrosion inhibitors for mild steel in 1 M HCl solution was done using various techniques such as weight loss, potentiodynamic polarization and electrochemical impedance spectroscopy (EIS) measurements. It was revealed that inhibition was concentration dependent as inhibition efficiency (IE) increases with the increase in the inhibitor concentration. Potentiodynamic polarization measurement indicated that the inhibitors act as “mixed-type” inhibitors with predominant anodic inhibition. EIS measurement indicated that the corrosion of mild steel in the absence and presence of inhibitor was mainly controlled by charge transfer process. The Randles-CPE model has been used as the equivalent circuit throughout this study. The optimum concentration obtained from all tests was at 1000 ppm (0.1 % wt). Temperature studies revealed that the corrosion rate of mild steel in the absence and presence of both inhibitors increases exponentially with temperature. Adsorption isotherm determination revealed that the inhibitor follows the Langmuir adsorption model. Surface analysis via SEM portrayed that there was a significant morphological improvement of mild steel surface in the presence of the inhibitor. The calculated

value of free energy of adsorption, ΔG_{ads} and potential zero charge (PZC) for the inhibitors indicate that the inhibition mechanism process was spontaneous and the inhibitors were physically adsorbed (physisorption) onto the mild steel surface.

**UNCARIA GAMBIR SEBAGAI PERENCAT KAKISAN SEMULA JADI BAGI
KELULI LEMBUT DI DALAM LARUTAN BERASID**

ABSTRAK

Uncaria gambir, tumbuhan herba asli dari Asia Tenggara telah dicirikan dan dikaji sebagai perencat kakisan keluli lembut dalam medium berasid. Kajian menunjukkan bahawa ekstrak etil asetat memberikan kandungan tanin terkondensasi, fenol dan flavonoid tertinggi berbanding ekstrak dari bahan pelarut yang lain. Kajian secara kuantitatif menggunakan HPLC telah menunjukkan bahawa lebih 80 % (berat) dari ekstrak gambir mengandungi katekin. Kesan ekstrak gambir daripada pelarut etil asetat dan (+)-catekin hidrat sebagai perencat kakisan bagi keluli lembut di dalam larutan 1 M HCl telah dijalankan menggunakan pelbagai teknik seperti penentuan kehilangan berat, pengukuran kekutuban potensiodinamik dan pengukuran spektroskopi elektrokimia impedans (EIS). Kajian menunjukkan bahawa perencatan tersebut adalah bergantung kepada kepekatan dimana keberkesanan perencatan (IE) meningkat dengan peningkatan kepekatan perencat. Pengukuran kekutuban potensiodinamik menunjukkan bahawa perencat tersebut bertindak sebagai perencat jenis campuran dengan kesan perencatan anodik yang paling dominan. Pengukuran EIS telah menunjukkan bahawa pengaratan keluli lembut dalam ketidak hadiran atau kehadiran perencat adalah secara amnya dikawal oleh proses pertukaran cas. Model Randles-CPE telah digunakan sebagai litar yang bersesuaian sepanjang kajian ini. Kepekatan optimum yang diperoleh daripada kesemua ujian adalah pada 1000 ppm (0.1 % berat). Kajian suhu menunjukkan bahawa kadar kakisan keluli lembut dalam ketidak hadiran dan kehadiran kedua-dua perencat meningkat secara eksponen dengan suhu. Penentuan isoterma penjerapan menunjukkan bahawa perencat tersebut mengikuti model penjerapan Langmuir. Analisis permukaan melalui SEM telah

menggambarkan bahawa terdapat pemulihan morfologi yang signifikan pada permukaan keluli lembut dalam kehadiran perencat. Nilai tenaga bebas penjerapan, ΔG_{ads} dan keupayaan cas sifar (PZC) yang dikira bagi perencat tersebut menunjukkan bahawa proses mekanisma perencatan yang berlaku adalah secara spontan dan terjerap secara fizikal (fizik-jerap) pada permukaan keluli lembut.

CHAPTER 1

INTRODUCTION

1.1 Introduction to Corrosion

Since the human existence, people have witness natural disaster around the world. One of the natural occurring disasters that still happen nowadays is corrosion. Corrosion or mostly known as rust were derived from Latin words ‘*rodere*’ which means gnawing and ‘*corrodere*’ which means gnawing into pieces (Sastri *et al.*, 2007a; Davis, 2000). Even though there are many terms that explain this phenomenon, but the fact is corrosion will cause physical damage, destroys the lustre and beauty of an object and thus shortens their life. An essay wrote by a Roman philosopher Pliny (AD 23-79) entitled “*Ferrum Corrumptar*” was one of the earliest manuscript recorded that tells about the physical damage of an iron in a period of time.

Previously, there were only few scientist who show some interest to study the corrosion phenomenon until Robert Boyle describe about the corrosion mechanism in his essay “*Mechanical Origin of Corrosiveness*” (Zaki Ahmad, 2006a; Sastri *et al.*, 2007a). Early in 19th century, the corrosion concept was explained in more detail from the electrochemistry perspective. In the year 1833, Michael Faraday established a quantitative relationship between chemical action and electric current. This theory has been used to explain the mechanism that happened in corrosion process.

Faraday's first and second laws are the basis for calculation of corrosion rates in metal (Walsh, 1991).

1.1.2 Corrosion in definitions

Corrosion process occurs in nature like any other natural disasters. The term corrosion can leads us into many definitions. Generally, corrosion will form a solid wastage on the metal surface when metal is being exposed in reactive environment.

According to Fontana (1986), corrosion is the deterioration of materials as a result of reaction with its environment. Corrosion also is the destructive attack of a metal by chemical or electrochemical reaction with environment (Uhlig, 1985). Despite of all its different definitions, corrosion is basically the result of interaction between materials and their environment. Some of the typical corrosive environments are (Zaki Ahmad, 2006a):

- Air and humidity
- Fresh, distilled, salt and marine water
- Acids and alkalies
- Soil, steam, gases

Nowadays, corrosion is not confined to metals and alloys alone, but it also now encompasses with all types of natural and man-made material for example biomaterials and nanomaterials. The scope of corrosion is consistent with the revolutionary changes in materials development witnessed in recent years.

1.1.3 Corrosion of iron

Irons play an important role in the industrial sectors nowadays. Problems that mostly encountered by the industrial sectors are corrosion of metals. The driving force that causes iron to corrode is natural consequence of their temporary existence in ionic form (thermodynamically unstable). In order to produce irons starting from naturally occurring minerals and ores, it is necessary to provide a certain amount of energy (Fig. 1.1). It is therefore only natural that when these irons are exposed to their environments, they would revert back to original state in which they were found (Roberge, 2008a; Zaki Ahmad, 2006a).

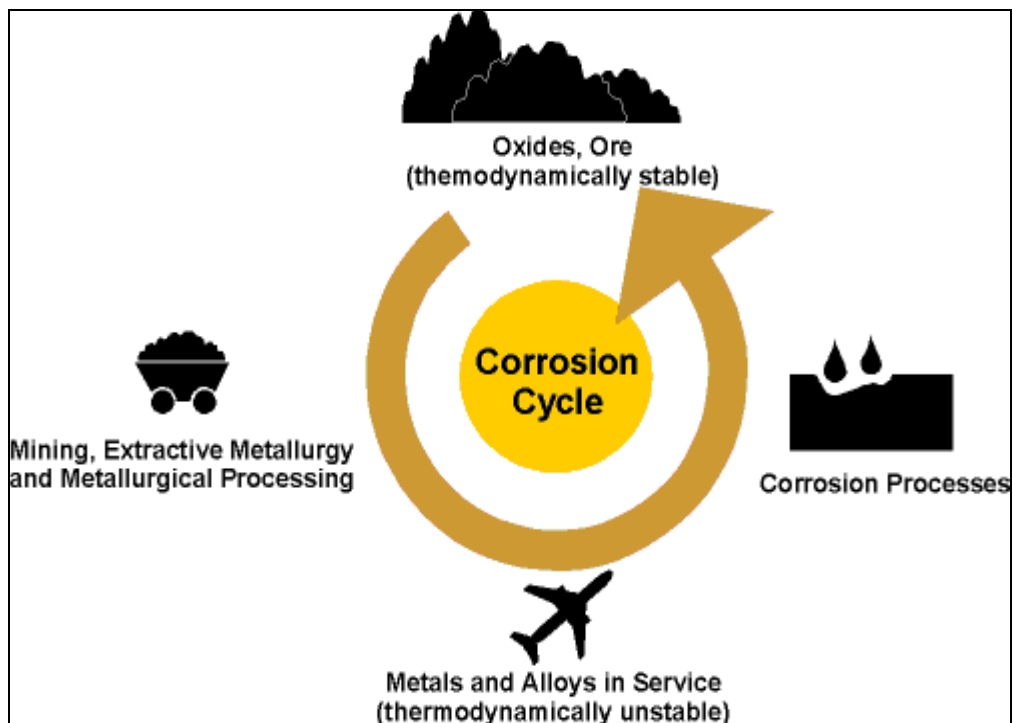


Figure 1.1: The corrosion cycle of steel.

In the presence of water and oxygen, metallic iron is thermodynamically unstable and corrosion proceeds according to the electrochemical mechanisms (Figure 1.2). As many electrochemical processes, the redox reaction of corrosion occurs both in anodic and cathodic terminal side of the metal surface. More than one oxidation and reduction process may occur during the process.

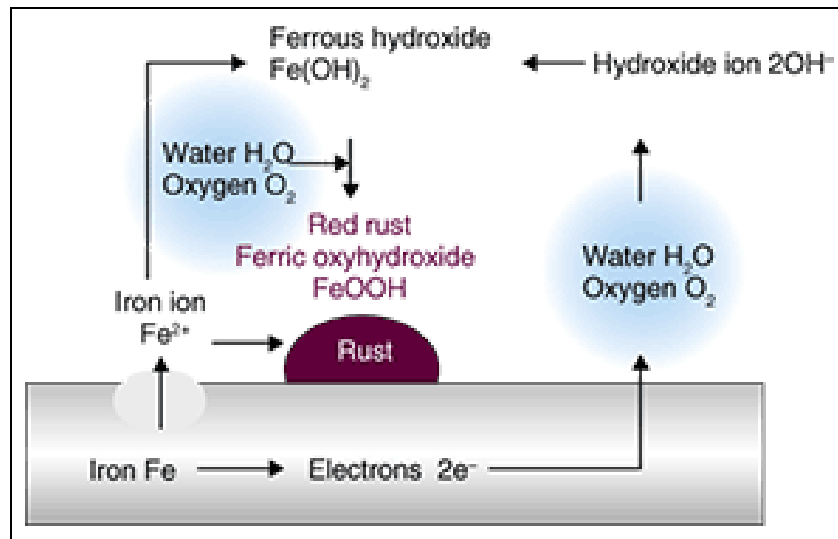
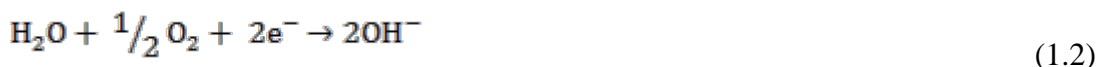


Figure 1.2: Electrochemical mechanism of corrosion of iron.

In the initial stage, iron is oxidized at the anode terminal to dissolve Fe^{2+} :



Oxygen is reduced at the cathode terminal to form OH ions:



The cathodic reaction represented by Equation 1.2 exemplifies corrosion in natural environment where corrosion occurs at nearly neutral pH values (Kruger, 2001).

In de-aerated or acidic solution, the cathodic reaction is (Sheir *et al.*, 1994):



If there is no oxidation or reduction occurs, the overall corrosion reaction is of course the sum of the cathodic and anodic partial reactions. This will form insoluble iron (II) hydroxide or green rust:



The colour of Fe(OH)_2 , although white when the substance is pure, is normally green to greenish black because of incipient oxidation by air (Revie and Uhlig, 2008a). The unstable iron (II) ions can also further oxidize to produce stable iron (III) ions:



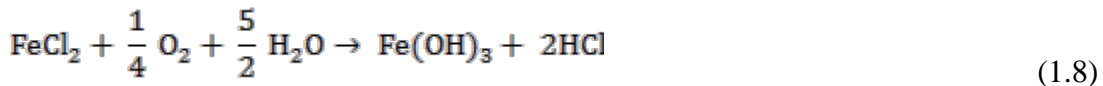
The iron (II) ions react with hydroxide ions to produce hydrated iron (III) oxides known as iron (III) hydroxides or ferric hydroxides or rust (reddish brown ferric hydroxide):



If iron comes into contact with hydrochloric acid, only the properties of the salt ferrous chloride and hydrogen gas can be detected (Groysman, 2010a):



The FeCl₂ will be oxidized by air transported through the anode channels to ferric hydroxide (Tamura, 2008):



The aging of Fe(OH)₃ leads to dehydration even in the presence of water and forms oxyhydroxides, FeOOH where no acid or base is consumed or generated and there would be no change in pH during the aging (Morgan and Stumm, 1981):



Or, the Fe(OH)₃ can slowly transform into a crystallized form written as Fe₂O₃.H₂O (red-brown in colour). There are many forms of corrosion products can be observed in the corrosion reaction of iron. Further oxidation and hydrolysis process in corrosion reaction of Fe(OH)₃ will produce α-FeOOH (goethite), β-FeOOH (akaganite), γ-FeOOH (lepidocrocite), Fe₃O₄ (magnetite) and so forth.

1.1.3 Consequences of corrosion

Corrosion of metal costs the Malaysian economy more than billions ringgit per year at current prices. For most industrialized nations, the average corrosion cost is 3.5-4.5 % of the gross domestic product (GDP) (Zaki Ahmad, 2006a; Davis, 2000). In a study of corrosion cost conducted jointly by C.C. Technologies Inc. USA, Federal Highway Agencies (FHWA) USA and National Association of Corrosion Engineers (NACE), the direct corrosion cost was estimated to be around 276 billion US dollars, approximately 3.1 % of the national gross domestic product (Zaki Ahmad, 2006a).

Of far more serious consequences is how corrosion affects our daily lives. Some consequences are economic and social, and cause the following (Davis, 2000):

- Replacement of corroded equipment.
- Preventive maintenance, for example, painting.
- Shutdown of equipment due to corrosion failure.
- Contamination of a product.
- Safety, for example, sudden failure can cause fire, explosion, release of toxic product and construction collapse.
- Health, for example, pollution due to escaping product from corroded equipment.

These costs can be reduced by broader application of corrosion-resistant materials and the application of best corrosion-related technical practices.

1.2 Corrosion protection

It is impossible for the corrosion scientist nowadays to completely eliminate corrosion. However, the types of electrochemical corrosion just described can be prevented or controlled by utilizing the current understanding of the principles underlying corrosion process. This understanding has been the basis for the development of a number of corrosion prevention measures. Three corrosion control

measures are based on the electrochemical driving force as shown in the Pourbaix diagram in Figure 1.3 (Kruger, 2001):

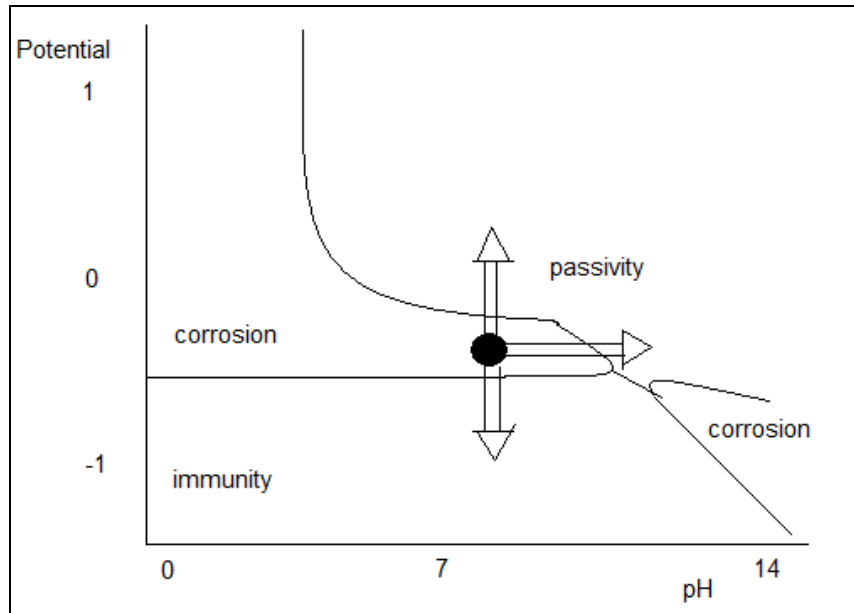


Figure 1.3: Pourbaix diagram for iron showing how corrosion protection can be achieved by using measures that bring a corroding system into either the immunity or the passivity region (Kruger, 2001).

The method chosen for corrosion prevention must consider the economical cost and the effectiveness since corrosion depends on both the specific water quality and material in a system. So, a particular method may be successful in one system, not in another (Singley *et al.*, 1985a). There are five primary methods of corrosion control that is material selection, coatings, inhibitors, cathodic protection and design (Singley *et al.*, 1985a; Kruger, 2001; Davis, 2000).

1.3 Corrosion inhibitors

Corrosion can be controlled by adding chemicals to the corrodent that form a protective film on the surface of a metal and provide a barrier between the water and the metal. This form of corrosion protection is called inhibition and the compound added to the system is called corrosion inhibitors. The inhibitors will reduce the corrosion rate but do not totally prevent it (Singley *et al.*, 1985a; Schweitzer, 2007b; Revie and Uhlig, 2008b; Kruger, 2001). The corrosion inhibitors are usually present in very low concentration (Groysman, 2010b; Sastri *et al.*, 2007b). According to Groysman (2010c), the concentration of corrosion inhibitors can be change from 1 to 15,000 ppm (0.0001 to 1.5 wt %). Besides, the inhibitors can be used at various ranges of pH, from acid, near neutral to alkaline. The most common and widely known use of inhibitors is their application in automobile cooling systems and boiler feedwaters.

It has been postulated that the inhibitors are adsorbed into the metal surface either by physical (electrostatic) adsorption or chemical adsorption. Physical adsorption is the result of electrostatic attractive forces between the organic ions and the electrically charged metal surface. Chemical adsorption is the transfer or sharing the inhibitor molecule's charge to the metal surface, forming a coordinate-type bond (Schweitzer, 2007b; Satri *et al.*, 2007b). Further explanations regarding the adsorption mechanism of inhibitors will be discussed on the next subchapter. The adsorbed inhibitor will reduces the corrosion rate of the metal surface either by retarding the anodic dissolution reaction of the metal by the cathodic evolution of hydrogen gas, or both.

According to Sastri *et al.* (2007b), a corrosion inhibitor can function in two ways. In some situations the added inhibitors can alter the corrosive environment into a noncorrosive or less corrosive species. In other cases, the corrosion inhibitor interacts with the metal surface and as a consequence, inhibits the corrosion of the metal. In the case of environment modifiers, the action and mechanism of inhibition is a simple interaction with the aggressive species in the environment, and thus reduce the attack of the metal by the aggressive species. Whilst, in the case of inhibitors which adsorb on the metal surface and inhibit the corrosion, there are two step namely: (i) transport of inhibitor to the metal surface and (ii) metal-inhibitor interaction.

In order to compare various corrosion inhibitors and select the most effective one for corrosion control, we have to calculate their efficiency (Groysman, 2010c; Schweitzer, 2007b; Roberge, 2008c; Sastri *et al.*, 2007b):

$$IE \% = \frac{CR_0 - CR_i}{CR_0} \times 100 \quad (1.10)$$

where CR_0 is the corrosion rate of metal in media without inhibitor, while CR_i is the corrosion rate of metal in media with inhibitor. The corrosion rate can be measured by any available method (weight loss or electrochemical method). According to Roberge (2008c), the efficiency of inhibitor increases with an increase of inhibitor concentrations until some point. Speaking about the efficiency, it is important to understand that there are some factors that can influence the efficiency of corrosion inhibitors. Groysman (2010c), stated that the common factors that influence the

efficiency of corrosion inhibitors are: the chemical position of aqueous solution, pH, flow rate, temperature and metal surface conditions (roughness, presence of corrosion product and other compounds). Inhibitors are most effective in definite pH range. For example, nitrites loses their effectiveness below a pH of 5.5 to 6.0, polyphosphate should be used between pH of 6.5 to 7.5, Zn-phosphate inhibitors are usually used at pH of 7.8 to 8.2.

Nowadays, there are various kinds of electrochemical instruments that commonly used to study the corrosion inhibition of a metal. Among those, the most popular once are gravimetric measurement or so called weight loss measurement, potentiodynamic polarization measurement and electrochemical impedance measurement. Numbers of research paper that have been published discuss about the metal corrosion inhibition behaviour using electrochemical measurements as stated above (Sherif and Park, 2006a; Obot *et al.*, 2009; Wahyuningrum *et al.*, 2008; Cheng *et al.*, 2007; Acharya and Upadhyay, 2004; Bouklah *et al.*, 2006; Morad and Kamal El-Dean, 2006; Talati *et al.*, 2005; Behpour *et al.*, 2007; Kustu *et al.*, 2007; Hosseini *et al.*, 2007; Hasanov *et al.*, 2007; Asan *et al.*, 2006).

1.3.1 The inhibitors

Generally, there are several classes of inhibitors, conveniently designated as follows (Schweitzer, 2007b; Revie and Uhlig, 2008b):

- Passivators, mainly chromates and nitrite.
- Organic inhibitors, including slushing compound and pickling inhibitors.
- Vapour-phase inhibitors.

Each inhibitor that being used for corrosion inhibition study will give different results depending on the environment or method employed. Even though passivator inhibitors are less expensive compare with other inhibitor, but most of corrosion scientists or engineers tend to use organic inhibitor as their main ingredient especially in paint or radiator coolant formulations. The advantages of organic inhibitor are because these materials build up a protective film of adsorbed molecules on the metal surface that provide a barrier to the dissolution of the metal in the electrolyte, not like other inhibitor which only effective for certain conditions.

Organic inhibitor can be divided into two categories, synthetic organic inhibitor or natural organic inhibitor. There is a lot of paper published in using synthetic compound as an inhibitor, such an example azole derivatives (Sherif and Park, 2006a; Obot *et al.*, 2009; Wahyuningrum *et al.*, 2008), carboxymethylchitosan (Cheng *et al.*, 2007), fluoroquinolones derivatives (Acharya and Upadhyay, 2004), pyridazine (Bouklah *et al.*, 2006), pyridine (Morad and Kamal El-Dean, 2006), Schiff bases derivatives (Talati *et al.*, 2005; Behpour *et al.*, 2007; Kustu *et al.*, 2007; Hosseini *et al.*, 2007; Hasanov *et al.*, 2007; Asan *et al.*, 2006) typtamine (Lowmunkhong *et al.*, 2010), quinine (Awad, 2006) and so forth. Unfortunately, even though these synthetic compounds showed very good anti-corrosive activity, but most of them are highly toxic to human and environment. Thus, synthetic

inhibitors can cause reversible (temporary) or irreversible (permanent) damage to internal organ as its presence in drinking water tank or in a pipeline. The toxicity of synthetic inhibitors maybe arises during the synthesis of the compound or while undergoing its application (Raja and Sethuraman, 2008). Hence, there is now been a trend to use natural product as green or so called “eco-friendly” inhibitor.

Some of the natural product inhibitors give different range of efficiencies, depending on the type of plant, metal and corrosive media used. Valek and Martinez (2007) used the leaves extract of *Azadirachta indica* as corrosion inhibitor for copper in sulphuric acid solution. Corrosion inhibition has also been studied for the extracts of olive leaves or *Olea europaea* for carbon steel (El-Etre, 2007), natural honey and black radish juice for tin (Radojcic' et al., 2008), *Ammi visnaga* or khillah for SX 316 steel (El-Etre, 2006), *Nypa fruticans* Wurmb for mild steel (Orubite and Oforka, 2004), *Sansevieria trifasciata* for aluminium (Oguzie, 2007), mangrove tannins (Rahim et al., 2008) and so forth.

1.3.2 Corrosion inhibition of mild steel in acidic solution

Acid solution are widely used in industry, the most important fields of application being acid pickling, industrial acid cleaning, acid descaling and oil well acidizing. As a result of aggressivity of acidic solution, the inhibitors are commonly used to reduce the corrosive attack on metallic materials. The development of inhibitors of steels in acidic solution has been the subject of great interest especially from the point of view of their efficiency and applications. Acids are classified into two parts

which is mineral acids (e.g. sulphuric acid, hydrochloric acid and phosphoric acid) and organic acids (e.g. acetic acid, malic acid and tartaric acid).

Most of corrosion inhibition studies were conducted in various concentration of acidic media since the use of acid solution in industrial sector is higher than others (alkaline or neutral) solution. Sulphuric acid and hydrochloric acid are aggressive towards the corrosion of iron and its alloys; hence most of corrosion chemists like to study the inhibitive properties in this environment. Eddy and Odoemelam (2009) reported about the corrosion inhibition behaviour of mild steel using ethanol extract of *Aloe vera* in sulphuric acid solution. Other research papers also use natural inhibitor as mild steel corrosion inhibitor, for example *Azadirachta indica* extract in hydrochloric acid and sulphuric acid solution (Oguzie, 2006), caffeic acid in sulphuric acid solution (de Souza and Spinelli, 2009), *Calendula officinalis* flower in hydrochloric acid solution (Subha and Saratha, 2006), *Calotropis procera* in sulphuric acid solution (Raja and Sethuraman, 2009), *Carica papaya* in sulphuric acid solution (Okafor and Ebenso, 2007) and many more.

1.3.3 Methods for corrosion inhibition study

In every study, there must be significant methods to prove any theory arises. In order to study more detail about the corrosion inhibition phenomenon, various methods has been developed from past until now. Previously, there are only few tests or methods employed to study the corrosion inhibition, but as the world of research keep wheeling, more and more methods were being manipulate to understand the

concept. Such methods are weight loss measurement, gasometric evaluation, potentiodynamic polarization measurement and electrochemical impedance spectroscopy (EIS). Surface and elemental analysis for example scanning electron microscope coupled with energy dispersive X-ray (SEM-EDX), X-ray diffraction spectroscopy (XRD), atomic force microscope (AFM) and X-ray florescence spectroscopy (XRF) are sometimes used to explain the surface morphology of metal and the formation of protective layer on metal surface. Below are few methods that commonly used in corrosion inhibition study.

1.3.3.1 Weight loss measurement

Weight loss measurements are considered as the simplest way to study corrosion phenomenon. Some refer it as gravimetric measurement (Okafor and Ebenso, 2006; Bendahou *et al.*, 2006). It gives useful information about the average corrosion rate over certain time period. In weight loss measurement, metal are usually being hanged or stand in a beaker that is loaded with corrosive medium and often covered with aluminium foil to avoid contamination and evaporation (Figure 1.4).

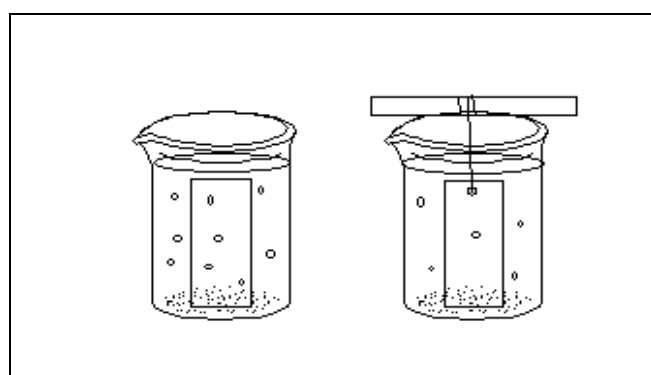


Figure 1.4: Typical weight loss measurement setup with metal being stand (left-hand side) and hanged (right-hand side).

There are certain things that we have to consider before undergo weight loss measurement. For example, the dimension or the size of metals, volume of electrolyte, pre-treatment before and after the test and time immersion. There is no restriction for the dimension of mild steel. El-Etre (2006) used a dimension of 2 cm x 5.6 cm x 0.2 mm (total surface area was 25 cm²) for his SX 316 steel while Valek and Martinez (2007) used a dimension of 4 cm x 5 cm x 3 mm (total surface area was 60 cm²) for their studies. Volume of electrolyte or solution that is used for the weight loss study must be sufficient in order to obtain a complete immersion of metal.

The pre-treatment of metal before and after weight loss test is important in order to get a precise value of inhibition. Metal surface is usually being treated before it is used in weight loss test. In this case, metal surface is been polished with emery paper or silicon carbide (SiC) paper from the most rough to less rough grade using a grinder polisher in order to obtain like a “mirror” surface. Wet polishing is commonly associated with this treatment where water will act as a lubricant.

Moreover, cleaning process is also one of the important procedures in weight loss measurement. This can divide into two categories, mechanical and chemical cleaning. Mechanical cleaning leads to the removal of substance that is attached on metal surface. Some methods used are scrubbing, scraping, sonicate, and brushing. While chemical cleaning is used to remove any material that forms or already exist on metal surface using suitable chemical solution. Examples of chemical solution used in chemical cleaning are acetone (El-Etre, 2006; Subha and Saratha, 2006; Raja

and Sethuraman, 2009), alcohol (Oguzie, 2006; Valek and Martinez, 2007) and ASTM G1-90 or known as Clarke's solution (Singh and Kumar, 2003).

Time of immersion is another thing that we have consider while studying weight loss test. Time that is fixed in weight loss measurement is the time which gives the maximum corrosion rate.

1.3.3.2 Potentiodynamic polarization measurement

Polarization studies have been primarily laboratory electrochemical technique to study corrosion phenomena, especially pitting and passivity, by disturbing the natural corrosion potential of a system, frequently by substantial amounts of volts and measuring the external current flowing (Schweitzer, 2007c; Jain, 2010b). The characterization of a metal specimen is done via current-potential relationship (Jain, 2010b). According to Perez (2004a), polarization is a process when the electrode reaction are assumed to induced deviations from equilibrium due to the passage of an electrical current through an electrochemical cell, causing a change in the working electrode (WE). The specimen is polarized to within ± 25 mV of the corrosion potential (E_{corr}) as the dependence of current with potential in vicinity of corrosion potential is linear (Zaki Ahmad, 2006b). The term E_{corr} can be defined as the potential at which the rate of oxidation is exactly equal to the rate of reduction (Jain, 2010b). In general, the electrochemical and chemical rates of reaction due to anodic or cathodic overpotentials can be predicted using both Faraday (Eq. 1.12) and Arrhenius (Eq. 1.13) equation respectively (Perez, 2004a):

$$R_F = \frac{iA_{wj}}{zF} \quad (1.12)$$

$$R_A = \gamma_a \exp\left(-\frac{\Delta G^*}{RT}\right) \quad (1.13)$$

where i is applied current density ($A \text{ cm}^{-2}$), A_{wj} is the atomic weight of species j (g mol^{-1}), z is the oxidation state or valence number, γ_a is the chemical reaction constant and ΔG^* is the activation energy or free energy change (J mol^{-1}).

At equilibrium, Faraday's and Arrhenius rate equations become equal ($R_F = R_A$) and consequently the current density becomes:

$$i = \gamma_a \exp\left(-\frac{\Delta G^*}{RT}\right) \quad (1.14)$$

On the other hand, if an electrode is polarized by an overpotential under steady-state conditions, then the rate of reaction are not equal ($R_F \neq R_A$) and consequently, the forward (i_f , cathodic) and reverse (i_r , anodic) current density components must be defined in terms of the free energy change ΔG deduce from Figure 1.5 where k'_f and k'_r are the forward and reverse rate. Hence;

$$i_f = k'_f \exp\left(-\frac{\Delta G_f^*}{RT}\right) \quad (\text{cathodic}) \quad (1.15)$$

$$i_r = k'_r \exp\left(-\frac{\Delta G_r^*}{RT}\right) \quad (\text{anodic}) \quad (1.16)$$

$$\text{and, } \Delta G_f^* = \Delta G_f - \alpha z F \eta_c \quad (1.17)$$

$$\Delta G_r^* = \Delta G_r + (1-\alpha)z F \eta_a \quad (1.18)$$

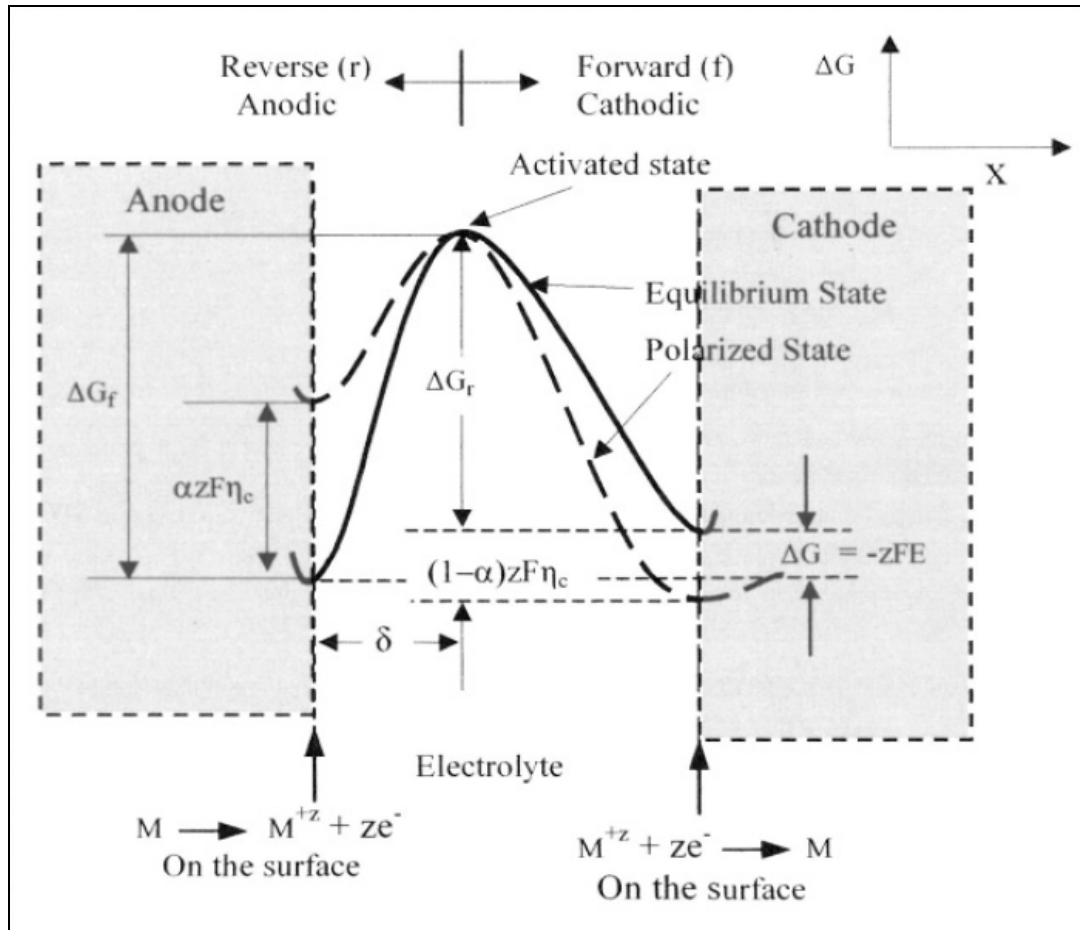


Figure 1.5: Schematic activation free energy distribution (Perez, 2004a).

α is the symmetry coefficient, F is the Faraday's constant and η is the potential of the reaction or polarization (for both cathodic and anodic). For a cathodic case, the net current and the overpotential are $i = i_f - i_r$ and η_c respectively. Substituting equation (1.15) and (1.16) into this expression yields the net current density in a general form:

$$i = k'_f \exp\left(-\frac{\Delta G_f^*}{RT}\right) \exp\left(\frac{\alpha zF\eta}{RT}\right) - k'_r \exp\left(-\frac{\Delta G_r^*}{RT}\right) \exp\left(-\frac{(1-\alpha)zF\eta}{RT}\right) \quad (1.19)$$

From which the exchange current density is deduced as:

$$i_o = k'_f \exp\left(-\frac{\Delta G_f^*}{RT}\right) = k'_r \exp\left(-\frac{\Delta G_r^*}{RT}\right) \quad (1.20)$$

Substituting equation (1.20) into (1.19) for one-step reaction yields the well known **Butler-Volmer equation** for polarizing an electrode from the open circuit potential E_o under steady-state conditions:

$$i = i_o \left\{ \exp\left(\frac{\alpha zF\eta}{RT}\right)_f - \exp\left(-\frac{(1-\alpha)zF\eta}{RT}\right)_r \right\} \quad (1.21)$$

where $\eta = E - E_o$ and E is the applied potential.

If the overpotential is large and positive ($\eta > +0.052$ V), the second term in equation (1.21) can be neglected (Jain, 2010c):

$$i = i_a = i_o \left\{ \exp\left(\frac{\alpha zF\eta}{RT}\right)_f \right\} \quad (1.22)$$

If the overpotential is large and negative ($\eta < -0.052$ V) the first term in equation (1.21) can be neglected:

$$i = i_a = i_o \left\{ \exp \left(- \frac{(1-\alpha)zF\eta}{RT} \right) \right\} \quad (1.23)$$

Taking the logarithms in equation (1.22):

$$\ln i_a = \ln i_o + \frac{\alpha z F \eta}{RT}$$

$$\ln \left(\frac{i_a}{i_o} \right) = \frac{\alpha z F \eta}{RT}$$

$$\eta = \frac{RT}{\alpha z F} \ln \left(\frac{i_a}{i_o} \right)$$

or,

$$\eta_a = \frac{2.303RT}{\alpha z F} \ln \left(\frac{i_a}{i_o} \right)$$

Then, by assuming that $\eta_a = \beta_a \log(i_a/i_o)$ and $\eta_b = \beta_c \log(i_c/i_o)$:

$$\beta_a = \frac{2.303RT}{\alpha z F} \quad (1.24)$$

$$\beta_c = \frac{2.303RT}{(1-\alpha)zF} \quad (1.25)$$

β_a and β_c are known as **Tafel slope**. These equations are used to calculate the anodic and cathodic current slope (Figure 1.6).

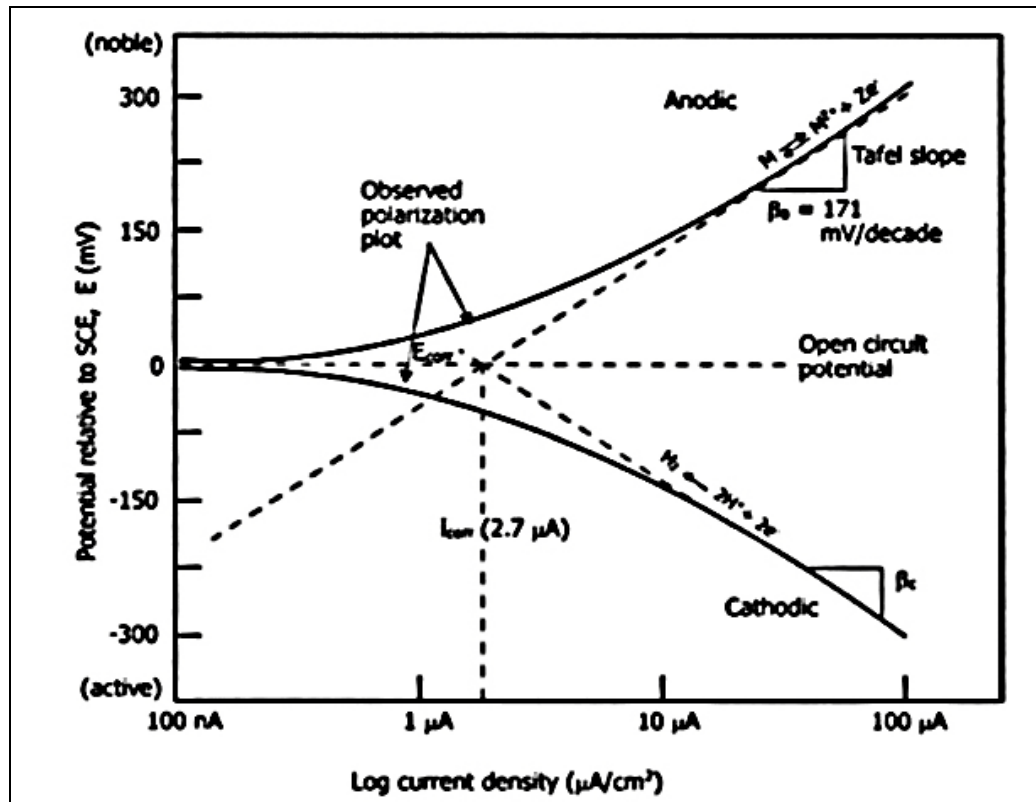


Figure 1.6: A hypothetical Tafel plot (Zaki Ahmad, 2006c).

Polarization resistance or so called linear polarization is usually being used in potentiodynamic polarization measurement. This technique is quick and reliable. According to Zaki Ahmad (2006c), polarization resistance (R_p) of a corroding metal is defined Ohm's Law as the slope of a potential (E) versus current density ($\log i$) plot at the corrosion potential (E_{corr}). Here, $R_p = (\Delta E / \Delta I)$ at $\Delta E = 0$. By measuring this slope, the rate of corrosion can be measured. The correlation between i_{corr} and slope (dE/dI) is given by:

$$R_p = \frac{\Delta E}{\Delta I} = \frac{\beta_a \beta_c}{2.303 i_{corr}(\beta_a + \beta_c)} \quad (1.26)$$

where β_a and β_c are Tafel slope.

There are three types of inhibitor that we can observe in potentiodynamic polarization test, which is cathodic inhibitor, anodic inhibitor and mixed inhibitor. Cathodic inhibitors inhibit the hydrogen evolution in acidic solution or the reduction of oxygen in neutral or alkaline solutions. It is also observed that the cathodic polarization curve is affected when a cathodic inhibitor is added to the system. Substances with high overpotential for hydrogen in acidic solutions and those that form insoluble products in alkaline solution are generally effective cathodic inhibitors. Anodic inhibitors are generally effective in the pH range of 6.5 to 10.5 (near neutral to basic). Basically, oxyanions are very effective anodic inhibitors. Those oxyanions are thought to play a role of repairing the defects in the passive metal oxide film on the metal surface. Mixed type of inhibitors is generally represented by organic compounds. Irrespective of type of inhibitor, the inhibition processes involve transport of inhibitor to the metal site followed by interaction of the inhibitor with the surface of the metal, resulting a protection (Sastri *et al.*, 2007b).

1.3.3.3 Electrochemical impedance spectroscopy (EIS)

Electrochemical impedance spectroscopy (or AC impedance) is a now well established laboratory technique used to determine the electrical impedance of metal-electrolyte interface at various AC excitation frequencies (Schweitzer, 2007c). Impedance measurements combine the effect of DC resistance with capacitance and inductance. Furthermore, the AC impedance is capable of characterizing the corrosion interface more comprehensively in lower conductivity solution or high-resistivity coatings (Schweitzer, 2007c; Revie and Uhlig, 2008c). In an alternating

circuit, impedance determines the amplitude of current for a given voltage and the proportionality factor between voltage and current (Revie and Uhlig, 2008c; Groysman, 2010d). The response of an electrode to alternating potential signals of varying frequency is interpreted on the basis of circuit models of the electrode or electrolyte interphase (Revie and Uhlig, 2008c; Perez, 2004b).

In DC theory, resistance R is defined by Ohm's Law:

$$E = IR \quad (1.27)$$

where I is the current (A) and E is the potential (V). Using the Ohm's law, one can apply a DC potential to a circuit and measure the resulting current, from which the resistance can be calculated (Zaki Ahmad, 2006b; Perez, 2004b; Groysman, 2010d).

In AC theory:

$$E = IZ \quad (1.28)$$

Here, Z is the magnitude of the impedance containing elements of an equivalent circuit, such as capacitors and inductors. Capacitors oppose or impede the current flow (Perez, 2004b). AC currents and voltages are vector quantities. Impedance can be expressed as a complete number where the resistance is the real component and combined capacitance and inductance is the imaging component (Zaki Ahmad, 2006b). The resulting vector for impedance is:

$$Z_{\text{total}} = Z' + Z''j \quad (1.29)$$

where Z' is the real impedance, Z'' is the imaginary impedance and j is $\sqrt{-1}$. The absolute magnitude of impedance is:

$$|Z| = \sqrt{(Z')^2 + (Z'')^2} \quad (1.30)$$

and,

$$\tan \theta = \frac{Z'}{Z''} \quad (1.31)$$

When the opposition to the current is capacitive resistance, the current leads the applied voltage in phase angle. But when the opposition to current flow is inductive reactance, the current lags behind the voltage in phase angle (Zaki Ahmad, 2006b). The phase angle (θ) is the difference between points on x-axis where current and voltage curve amplitudes are zero (Figure 1.7). Table 1.1 shows the transfer function for resistors, capacitors and inductors.

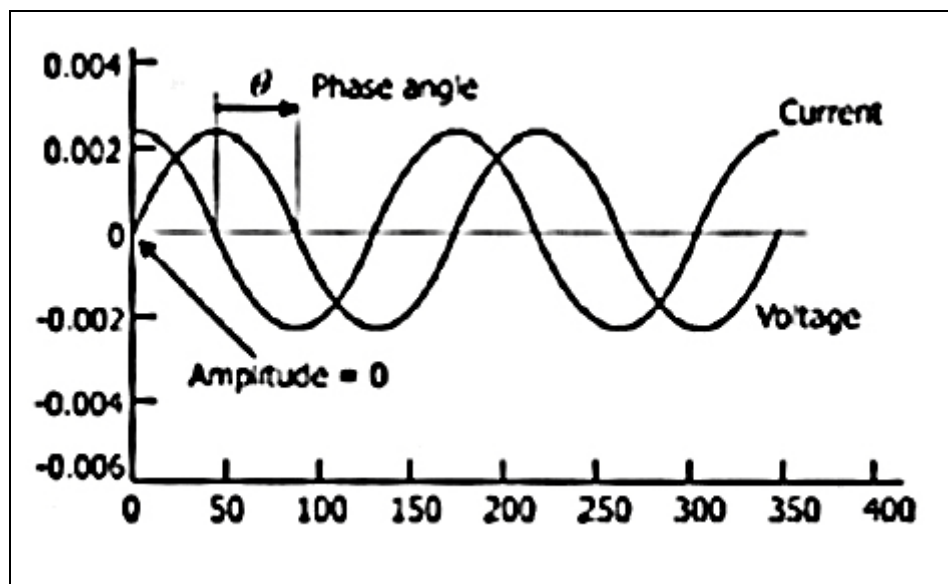


Figure 1.7: The voltage-current phase angle (Zaki Ahmad, 2006b).